Computations on Neutral Beam Injection Heating, Ripple Recommendations and Varying Compression Ratio in ZEPHYR

O. Gruber, K. Lackner, G. Lister

IPP 1/199 April 1982

Reprint of ZEPHYR-Report No. 16 of Aug. 1980.

MAX-PLANCK-INSTITUT FÜR PLASMAPHYSIK

8046 GARCHING BEI MÜNCHEN

MAX-PLANCK-INSTITUT FÜR PLASMAPHYSIK

GARCHING BEI MÜNCHEN

Computations on Neutral Beam Injection Heating, Ripple Recommendations and Varying Compression Ratio in ZEPHYR

O. Gruber, K. Lackner, G. Lister

IPP 1/199 April 1982

Reprint of ZEPHYR-Report No. 16 of Aug. 1980.

Die nachstehende Arbeit wurde im Rahmen des Vertrages zwischen dem Max-Planck-Institut für Plasmaphysik und der Europäischen Atomgemeinschaft über die Zusammenarbeit auf dem Gebiete der Plasmaphysik durchgeführt.

IPP 1/199

O. Gruber
K. Lackner
G. Lister

Computations on Neutral Beam Injection Heating, Ripple Recommendations and Varying Compression Ratio in ZEPHYR

April 1982 (in English)

Abstract

Transport calculations show that the ion thermal transport losses limit the allowed toroidal field ripple in the uncompressed state of ZEPHYR to about ± 1.5 % as compared to the actual value of ± 6 % for 16 toroidal field coils. Changing the design to a 20 coil set results in a ripple with ± 3.4 % and a steeper radial decrease towards the plasma centre, so that the ripple losses can be compensated by a 1 MW increase in the neutral injection power.

These results are compatible with particle trajectory calculations of the fast ion losses and the central plasma heating with neutral injection. The necessary conditions for ignition can be attained with a total heating power of 25 MW provided the ripple can be reduced to ± 1 % for 16 toroidal field coils, in which case the energy losses could be kept below 30 %. For the 20 coil set with ± 3.4 % ripple higher losses are expected and calculations are currently under way. The proposed 160 keV beams would give 15 to 20 % more power to the central region of the plasma compared with 120 keV beams.

As the ripple decreases rapidly with the major radius its influence could be significantly reduced by lowering the compression ratio. Transport calculations reported here indicate a respective reserve in our design.

1. Introduction

In order to ignite the proposed ZEPHYR experiment /1/ with a compression ratio of 1.5 by neutral injection (NI) with 160 keV deuterons a heating power of about 20 MW, a pulse length of 1 s and power fractions of 60 : 20 : 20 for the full, half and one-third energy components have been found to be sufficient for an Alcator-Intor transport model /2, 3/. These calculations have been done without reference to the effect of magnetic field ripple caused by the discrete numbers of toroidal field (TF) coils in the tape wound coil design or by the neutral beam injection port holes in the Bitter coil case, respectively. The adverse effects of the toroidal field asymmetry are due to the trapping of fast ions in the local mirrors such that they drift out of the plasma or an induced random displacement of banana orbits and lead to a

- enhanced bulk-ion thermal transport
- loss of ripple trapped and banana trapped injected beam ions
- depletion of the high energy tail of the thermal ion distribution
- loss of trapped fusion alpha particles.

In contrast to the beam injected particles the α - particles and the fast thermal particles are born isotropically and near the plasma centre. Moreover, this contribution to the plasma heating and fusion rate is important only in the compressed plasma where the coil ripple is small ($\pm$ 0.1 %) and the associated losses should be negligible. The ripple coming from the magnetic vessel structure has to be considered later on. The ion thermal transport is tolerable in the compressed plasma due to the insignificant ripple, but limits the allowed ripple in the uncompressed state as is shown in chapter 2 by 1-d transport calculations. The effects of TF ripple on neutral injection in the uncompressed plasma and the penetration problem with lower injection energies and different energy mixes are treated with particle trajectory calculations in chapter 3 and 4, respectively. For a given toroidal field coil geometry the ripple requirements can be facilitated by reducing the compression ratio; the resultant gain has to be traded off against the beneficial effects of stronger compression described in chapter 5.

2. Enhanced Ion Thermal Transport with TF Ripple

The discrete numbers of toroidal field coils or the NI port holes yield a toroidal field asymmetry and additionally trapped particles contributing to an enhanced thermal diffusivity. Especially in the uncompressed plasma a high peak to average ripple δ exists, whose radial (r), poloidal (θ) and toroidal (ϕ) variation can be described by

$$B = \frac{B_o R_o}{R} (1+\delta)$$

$$\delta(r, \theta, \phi) = [\delta_o + (\delta_a - \delta_o) \frac{r^m}{a^m}] e^{-\beta \theta^2} \cos N\phi$$

B is the toroidal field and R_o the major plasma radius. Comparing this expression with the constant ripple contours of the tape wound TF coil with N = 16 toroidal coils given in Fig. 1 /4/ yields a good fit over the uncompressed plasma region for $\delta_o = 0.2$ %, $\delta_a = 6.4$ %, m = 3 and ß = 0.36.

The influence of the field ripple via ion heat conduction on the average ion temperature at the end of the NI heating just prior the adiabatic compression is shown in Fig. 2 for two densities and two NI heating powers. At the higher density of $1.5 \cdot 10^{14}$ cm^{-3} the plasma ignites after the compression with a temperature slightly below 5 keV before compression, while for the lower density of 10^{14} cm^{-3} a $\langle T_i \rangle \approx 10$ keV before compression is needed ($\langle T_e \rangle \approx 6.5$ keV, hot ion mode). Results shown here were obtained with the 1-d transport code WHIST /5/ where internal sawteeth are included but no impurities /3/ or ripple induced losses of the beam ions. The density profile is kept nearly parabolic with an edge density of 1/10 of the central density by specifying a cold-ion source distribution. The main parameters of the precompression phase are

major radius R_o = 202.5 cm minor radius a = 61 cm

toroidal magnetic field B_o = 61 kG plasma current I = 2.4 MA.

The ion heat conduction model used consists of the neoclassical term and three contributions to the ripple induced drift. The ripple trapping term /6/ describes particles trapped in the TF minimum between the coils and drifting toroidally

$$\chi_i^{RT} \sim \frac{\delta(r)^{3/2} T_i^{7/2}}{R^2 n B^2} G(r, \theta, N)$$

The factor G takes into account both toroidal effect and the poloidal variation of the depth and shape of the local magnetic wells /7/ and increases approximately with $(\delta(r)\, N\, q\, A)^2$ for ZEPHYR parameters. The ripple plateau term /8/ describes toroidally trapped ions passing through the ripple with a sufficiently small $v_{\parallel}$ value to suffer one effective collision as they traverse one ripple phase

$$\chi_i^{RP} \sim \frac{\delta(r)^2\, T_i^{3/2}}{B^2} \quad \frac{R\, N\, q^2}{r^2} \quad \int_0^{2\pi} \frac{\delta(\theta)^2\, d\theta}{2\pi}$$

χ_i^{RP} is independent of the ion collision frequency. Toroidally trapped particles executing banana orbits experience an additional drift of their banana guiding centre and give a banana diffusion term which has been calculated by two authors yielding

$$\chi_i^{BD}(1) \sim \frac{\delta(r)^2\, T_i^{7/2}}{n\, B^2} \quad \frac{r^{3/2}}{R^{7/2}} \quad \frac{N^2}{(m+2)^2}\, q^2 \qquad /5/$$

and

$$\chi_i^{BD}(2) \sim \frac{\delta(r)^2\, T_i^{7/2}}{n\, B^2} \quad \frac{1}{R^{3/2} r^{1/2}} \quad \frac{1}{N q} \quad \int_0^{2\pi} \frac{\delta(\theta)^2\, d\theta}{2\pi} \qquad /9/$$

Both these expressions are (for the ZEPHYR design) much smaller than the other two terms, which are on the other hand larger than the anomalous electron heat conductivity (Alcator-Intor scaling) $\chi_e = \frac{6.25 \cdot 10^{17}}{n_e\,(cm^{-3})}$ cm^2/sec used.

The results show that the boundary ripple for a 16 TF coil system would have to be lowered to about $\pm$ 1.5 % as compared with the actual value of $\pm$ 6 % to render the ripple associated heat losses negligible. Only if higher heating powers are taken corresponding to a higher ignition parameter $(P_\alpha - P_{loss})/P_\alpha$ also higher ripple values are tolerable. This is shown for the higher density case with 16 MW heating power. It should be mentioned here that one has to add to the heating powers given in Fig. 2 about 2.5 MW for CX losses with the plasma neutrals and about 4 to 5 MW for impurity radiation losses /2,3/. We have found that the poloidal variation of δ is not critical for the maximum δ_a if $\beta > 0.3$, while the radial decrease of $\delta \sim \frac{r^m}{a^m}$ should not be too flat. A lower number of toroidal field coils corresponding to m = 2, for instance, allows only a $\delta_a = \pm 0.7$ %.

One possibility to lower the field ripple within the same coil geometry is an enhancement

of the TF coil number. Changing the ZEPHYR design to a 20 coil set changes both the ripple amplitude (δ_a = 3.4 %, δ_0 = 0.03 %) and its radial dependence (m = 3.6, ß = 0.5). Due to this stronger radial decrease of δ towards the plasma axis the obtained ripple is tolerable, if the remaining ripple losses are compensated by a 1 MW increase in the NI power. Additionally, the same post-compression plasma parameters can be achieved by varying the compression ratio between 1.5 and 1.4 with a corresponding lower ripple of δ_a = 1 %.

There are no difficulties with the ripple induced thermal transport in the compressed plasma, if the ripple requirements in the uncompressed plasma are already fulfilled. From the adiabatic scaling laws for a radial compression $k = \frac{R_{0,AC}}{R_{0,B.C}}$ and the thermal conductivities given above one obtains

$$\chi_i^{RT} \sim \delta^{7/2} k^{5/3}$$

$$\chi_i^{RP} \sim \delta^2$$

$$\chi_e \sim \frac{1}{k^2}$$

That means, for the same relation between χ_i^{Ripple} and χ_e as in the precompression plasma δ has to be lowered by $\delta \sim k^{-22/21}$ and $\delta \sim k^{-1}$ respectively, which is a very weak condition compared with actual ripple of Fig. 1.

3. Effect of TF ripple on NI Efficiency and Orbit Losses

Computational studies of the effect of TF ripple on the heating efficiency and loss rate of neutral beam injection have been done with a Monte-Carlo orbit following code /10/ both for the preliminary design value of ± 6 % and a reduced ripple of ± 1 %, using the spatial variation of the ripple corresponding to the original 16 coil design.
Plasma parameters have been obtained from the 1-d transport calculations /2,3/for both the beginning and end stages of the precompression phase of the experiment, when the density profiles are parabolic or rather flat respectively (see Fig. 3). The average density used is $1.5 \cdot 10^{14}$ cm^{-3} and the corresponding temperature profiles are parabolic like with $T_e = T_i$ = 8.7 keV on axis. These calculations have also been used to determin how much heating is required during the precompression phase to ensure ignition after the

adiabatic compression, when α-particle heating dominates the losses. The figure of merit used to correct the neutral injection power specifications for the ripple induced beam-ion orbit effects is ε , the fraction of injection power deposited within 40 % of the plasma minor radius, i.e. within 16 % of the plasma volume. Equal ε - values mean equal necessary heating powers for the same plasma parameters and to zero order equal impurity production due to wall loading. If the penetration or ε is inadequate a higher beam power must be used and the impurity influx may also be higher. For ε (0.4 a) = 0.2 ignition should occur if 16 MW of NI heating is applied assuming no plasma impurities, or 20 MW assuming 1 % iron or 3.5 % carbon to be present. These ε -values should be observed as results on PLT have shown that for substantial heating it was necessary to have $\varepsilon(0.3\ a) \geq 0.15$ /11/. To obtain these high values of ε in ZEPHYR with high line densities ($\sim 1.2 \cdot 10^{16}$ cm^{-2}) the beam particles must be injected at angles close to perpendicular in which case the fast ions deposited by the neutral beam are highly susceptible to the effects of field ripple. For all technically accessible injection angles the fast ions produced are trapped in "banana" orbits, at least until they have had sufficient Coulomb interactions to scatter them into "passing" particles. For this reason counter-injection cannot be considered because of the large energy losses resulting from unconfined orbits. Even for coinjected particles a large number of the banana trapped particles have mirror points in region where the field ripple is high and may be lost even though their initial pitch angle is sufficient to avoid immediate trapping in the ripple.

The proposed engineering design of the beam lines has been modelled as closely as possible in the calculations /12/. The main axis of each beam line is in the medium plane of the torus with a distance of 800 cm between the neutral particle source and the centre of the injection duct. The neutral particles emerge from a rectangular plane source, 40 cm x 10 cm. The beam lets are focused to the centre of the duct with a mean divergence of $\sigma = \pm 1.7^{\circ}$ in the vertical direction and $\pm 0.7^{\circ}$ in the horizontal direction with a Gaussian distribution exp ($-\theta^2/\sigma^2$). Thus some of the neutral particles will fail to pass through the duct (assumed to be a 40 x 20 or a 70 x 30 cm^2 rectangle, parallel to the beam force and located at a distance of 323 cm from the axis of the torus). Space limitations require that the injection angles between two adjacent sources must be separated by about 6°. We have considered mainly two beam

injection systems

160 keV with U : U/2 : U/3 power fractions 60 : 20 : 20

and 120 keV with U : U/2 : U/3 power fractions 75 : 16 : 9.

Fig. 4 shows the variation of the central heating efficiency ε as a function of the injection angle for the 160 keV system. Without toroidal field ripple ε is found to have a maximum at approximately 20° injection. For $\theta > 20°$ the increase of the central deposition with decreasing injection angle comes from the shift of the initial deposition of ions towards the plasma centre due to the smaller $\int n\,dl$ seen. No simple $\varepsilon \sim \exp(-\int n dr/E\cos\theta)$ law is found due to the following reasons. For a pencil beam in the torus midplane and neglecting orbit effects ε within a radius r_o is given by

$$\varepsilon = e^{\int_a^{r_o} \frac{\sigma_t n\,dr}{\cos\theta}} - e^{\int_a^{-r_o} \frac{\sigma_t n\,dr}{\cos\theta}}$$

σ_t is the cross section for ionization and CX of the injected neutral particles. For the higher energy components the total cross section becomes smaller $\sigma_t \sim \frac{1}{E}$ and the second term is no longer negligible. This effect is even stronger if an extended neutral beam with a smaller beam path outside the torus midplane and orbit effects are considered. The latter yield an increase of the central deposition compared with the birth ε value by about 40 %, as the co-injected particle orbits are shifted towards the plasma centre. Altogether for one energy component a dependence

$$\varepsilon = e^{-\text{const}/(E^{0.8}\cos\theta^*)}$$

has been found, where θ^* is the injection angle at $R_o + a/2$. Below 20° ε is decreasing again, as the widths of the banana orbits decrease with decreasing injection angle. Furthermore fast particles may be scattered on counter injection orbits, which are shifted towards the plasma boundary.

With a toroidal field ripple of 1 % at the plasma boundary the central deposition is reduced by about 25 % for injection angles less than 25° and drops to even lower values for a more tangential injection. The beam ions, although unaffected by the ripple at their point of origin,

become trapped by the main toroidal field at points where field ripple is also significant. For cases with field ripple of $\pm$ 6 % a further reduction in efficiency is found corresponding to a $\sim$35 % reduction at 24° injection angle compared with the zero ripple case.

The orbit losses of the fast ions are found to increase nearly linearly with the boundary ripple δ_a . Without TF ripple the losses are in the range of a few per cent due to banana losses. For the case considered in Fig. 5 ($\delta_a = \pm$ 1 %) ions are directly trapped in the ripple for injection angles $< 10^\circ$ and the increasing losses below 30° are due to scattering from banana orbits to ripple trapped orbits and additionally banana drift in the ripple induced mirrors. When $\delta_a = \pm$ 6 % direct ripple trapping occurs for angles $<20^\circ$ and losses subsequently become intolerably high. The effect of varying the poloidal "shaping factor" ß is quite marked - if ß is increased from 0.36 to 1.1 we find that for the 160 keV ions losses are reduced from 0.47 to 0.24. As expected, parabolic density profiles result in $\sim$15 % higher efficiencies and $\sim$ 35 % lower orbit losses than flat profiles, since the neutral particles are trapped nearer to the plasma centre.

These results indicate that the ripple associated with the preliminary design of the experiment is intolerable and one has to limit the ripple at the outer uncompressed plasma edge to about 1 % . This value is also found to limit the enhanced thermal transport of the bulk ions (see chapter 2). Calculations are currently under way using the ripple shape and amplitude resulting for a 20 TF coil concept. But even with the lowered ripple an injection energy of 160 keV, a nearly perpendicular injection between 8 ° and 25° and a compression ratio of the order $\sim$ 1.5 are necessary. Moreover, the total heating power has to be raised by about 25 % to get the necessary central heating power. There is a possibility for smaller compression ratios and subsequently lower boundary ripple values if the stronger contribution of the α - particle heating for higher initial densities is taken into account (see chapter 5). Additionally a reduced compression ratio can be compensated partly by an improved species mix with a higher full energy component and/or by increasing the NI pulse length. But this leads again to a higher wall loading.

4. Influence of the Injection Energy

For lower injection energies the heating power has to be raised according to $P \sim \frac{1}{\sqrt{U}}$ /3/ in order to obtain the same plasma parameters. This is due to the lower ε- values for the smaller injection energies and has been confirmed by the particle trajectory calculations. The enhanced impurity flows due to the higher wall loading are further increased by charge exchange losses ($\sim \frac{1}{U}$) and demand for even higher heating powers at lower energies or finally prevent ignition at all. In addition, if the electron thermal conductivity increases radially outwards much faster than given by the anomal scaling $\chi_e \sim \frac{1}{n_e}$ used in the codes more of the power deposited in the outer plasma is lost to the walls and does not serve as a heat bath. These problems demand therefore for a low power level and a central deposition of the heating power.

For a 120 keV injection system (with power fractions of 75 : 16 : 9 for the three energy components) the ε values are about 10 - 20 % lower than given for the 160 keV system in Fig. 4, whereas the ripple losses are the same as given in Fig. 5. A comparison between different injection energies is shown in Fig. 6, where the necessary portion of the full energy component is given to have an equal $\varepsilon = 0.2$ within 40 % of the plasma radius. There is also shown the necessary D^+ percentage in the ion source, where only 90 % of the max. neutralization efficiency for the D^+ ions has been taken into account. Only with the highest D^+ per centage of 85 % quoted till now, the injection energy can be lowered to 140 keV at most.

A compensation of the neutral beam heating with lower energies by higher compression ratios leads to a strong increase in machine size and costs for a fixed $\pm$ 1 % boundary ripple of the uncompressed plasma. If, for instance, the D^+ portion in the ion source is fixed to 80 %, the magnetic field energy increases typically by 50 % by changing from the 160 keV system to the 120 keV system (see Fig. 7). This field energy increase is much more expensive than the cost difference between the two injection systems.

5. Transport Calculations with Varying Compression Ratio

As the main field ripple decreases rapidly with major radius, decreasing the compression ratio offers a simple way to reduce the associated problems. The compression ratio affects the energy balance however also in several other ways : large values of it improve neutral beam penetration and increase the effect of adiabatic heating whereas reduced compression, on the other hand, implies that the heating phase of the plasma proceeds at larger values of $n\tau_E$ possibly resulting in an increased thermonuclear contribution to it. The BALDUR transport calculations /2/ reported in this section describe the trade-off between those latter, axisymmetric effects, so that corrections due to injected ion orbit losses and ripple enhancement of heat conduction have to be applied separately.

All cases reported here correspond to the same post-compression configuration as the ZEPHYR standard parameter set, and a post compression average density $\langle n \rangle = 3.6 \times 10^{14}$ cm^{-3}. The compression ratio, however, was varied between 1 and 1.75 by chosing appropriately pre-compression geometry and density scenario. Exactly perpendicular injection (no orbit losses are included in these calculations) of 18 MW total power into the plasma was assumed, abundant for reaching ignition for our standard transport model and compression scenario in the absence of impurities. A finite time for compression (100 msec) during which neutral injection is continued, was assumed. CX losses are taken into account.

The solid line in fig. 8 shows the results in the form of the $\langle \beta_t \rangle$ -value after compression as a function of compression ratio C for a 160 keV NI system with a pulse length (including the compression phase) of 1.1 sec and our standard spezies mix (0.6 : 0.2 : 0.2 of power) and transport model. The parameter $\langle \beta_t \rangle$ is a good measure of ignition probability in comparisons involving the same confinement law. It is found to increase monotonically with compression ratio: for values of C larger than 1.16 ($\langle \beta_t \rangle > 2.6$), ignition would be predicted by these calculations.

The improvement in $\langle \beta_t \rangle$ with increasing C was found to be even more pronounced for a heat conduction model including an additional improvement of confinement in the center but a degradation in the periphery like found in the PLT experiments. Calculations shown by the dashed line in fig. 8 use a law

$$n\chi_e = \frac{2 \cdot 10^{19}}{1 + 10\left(1 - \frac{r^2}{a^2}\right)^{3.5}}$$

corresponding to the radial variation observed in PLT, but a coefficient increased by a factor ~ 2 to yield the same ignition probability as our standard model for the reference conditions with C = 1.5. The ratio between the achieved $\langle \beta_t \rangle$ values at C = 1.75 and C = 1 under these conditions, is still considerably larger than in the case of the Alcator model. The absolute numbers in $\langle \beta_t \rangle$ are smaller for the case of a radially dependent $n\chi_e$-law, but as the profiles tend to be more peaked and as the efficiency of thermonuclear heating is particularly affected by the confinement in the center region, the ignition behaviour is comparable for $C \approx 1.5$. This is illustrated in Fig. 9, which gives the variation of the ignition parameter $(P_\alpha - P_{loss})/P_\alpha$, as monitored 0.7 sec after the end of compression, as a function of compression ratio for the two types of confinement law.

Several effects could be used to compensate the consequences of a reduced compression ratio. A significant improvement in $\langle \beta_t \rangle$ and ignition probability would result, if a better spezies mix could be realized in the neutral injection system. The comparison in fig. 10 between the performance of two systems with the same total power shows that an enhancement of the power fraction in the principal energy component from 60 % to 78 % could compensate for a reduction in compression ratio from 1.5 to 1.27. Such an improvement in neutral injector design (corresponding to 90 % D^+ ions in the source) is not expected on the time scale of interest for ZEPHYR: the results underline, however, the usefulness of further development in this direction.

In cases of reduced compression ratio, an improvement in ignition probability can also be gained by an increased pulse length of the neutral injection system, at least in the frame of the computational model used here, which e.g. does not include possible cumulative effects from impurity production. The benefit derives from the fact that at modest compression ratios, the contribution of α - particle heating leads to a continuous thermal runaway in the pre-compression state, as long as the additional heating system is active. The consequences of this effect are illustrated in fig. 11a, where the length of the neutral injection pulse

before compression was adjusted to correspond always to the same number of pre-compression electron energy confinement times. According to the scaling inherent in our standard heat conduction model, this implies a variation of pulse length as shown in fig. 11b, where for comparison`s sake, the absolute value was chosen identical to the one in our standard scenario for C = 1.5 (the neutral injection pulse length includes also the 100 msec for the compression phase which was taken to be the same in all cases). As can be seen from the comparison of fig. 4a, these scenarios lead to a considerably flatter dependence of ignition probability on compression ratio than those with fixed pulse length. Because of the dependence of these results on the computational model and the technological uncertainty in the pulse length enhancement within the ZEPHYR time frame, we do not plan to use this possibility as a standard scenario, but rather an interesting side-option to be tested if promising feasible.

The simplest trade-off for a modest decrease in compression ratio would be, however, an increase in neutral injection power. A quantitative decision can be made from a comparison of these requirements, with the variation of the ripple induced losses, which will decrease with decreasing compression ratio. Clearly a compromise in the region $1.4 < C < 1.5$ should be possible for the 20 coil design, carrying a penalty of less than 10 % in the injection power requirements as compared to a (hypothetical) case of a 16 coil configuration with C = 1.5 and $\delta_a = 1$ % at the uncompressed plasma boundary.

References

/1/ ZEPHYR Proposal for a Compact Ignition Experiment, IPP Study Group, January 1979, revised June 1979

/2/ K. Lackner, R. Wunderlich, Internal ZEPHYR Report 1 (1979), IPP 1/177
K. Lackner et al., Int. ZEPHYR Report 23 (1980)

/3/ O. Gruber, Internal ZEPHYR Report 7 (1979), IPP 1/178

/4/ Calculations were done by H. Preis (IPP) and W. Langton (MIT)

/5/ W.A. Houlberg, R.W. Conn, Proc. Topical Meeting on Improved Methods of Analysis of Nucl. Systems (1977)

/6/ N.A. Uckam, K.T. Tsang, J.D. Callen, ORNL-TM-5438 (1976)

/7/ R.J. Goldston, H.H. Towner, PPPL-1638 (1980)

/8/ A.H. Boozer, PPPL-1619 (1980)

/9/ A.H. Boozer, private communication

/10/ G. Lister, O. Gruber, Proc. Joint Grenoble-Varenna Symp. on Heating in Toroidal Plasmas (1980)

/11/ see, for instance, INTOR-report (1979), IAEA, Vienna (1979)

/12/ W. Herrmann et al., Internal ZEPHYR Report 29 (1980)

Figure Captions

Fig. 1 Constant TF ripple lines for the ZEPHYR design with 16 toroidal field coils. The plasma contours for the compressed and uncompressed plasma with a compression ratio of 1.5 are shown.

Fig. 2 Average ion temperature achieved after 1 s of NI for two values of injection power and particle density respectively as a function of TF edge ripple. The decrease in ion temperature for a smoother radial variation of the ripple $\sim \frac{r^m}{a^m}$ is shown for m = 2 compared with the standard design value m = 3.

Fig. 3 Radial electron density profiles characteristic for the beginning ("peaked") and the end ("flat") of the neutral injection phase for an average density of $1.5 \cdot 10^{14}$ cm^{-3}.

Fig. 4 Dependence of central energy deposition ε for the peaked profile (solid lines) and the flat profile (dashed lines) on injection angle at the plasma major radius $R_{o,B.C.}$ for a zero and $\pm$ 1 % ripple amplitude at the plasma boundary, respectively (160 keV NI system, m = 3, ß = 0.36).

Fig. 5 Dependence of orbit losses on injection angle at the plasma major radius $R_{o,B.C.}$ for the peaked and flat profile and 1% boundary ripple. The orbit losses with 6 % and zero ripple at $\theta = 24^{\circ}$ are shown for comparison (160 keV NI system m = 3, ß = 0.36).

Fig. 6 Necessary portion of the full energy component (solid line) and the corresponding D^+ percentage in the ion source (assuming 90 % of the maximum neutralization efficiency for the D^+ ions) as a function of the injection energy to get a central energy deposition $\varepsilon = 0.2$ without TF ripple.

Fig. 7 Necessary compression ratio and magnetic field energy as function of the injection energy for a fixed D^+ portion of 80 % in the ion source and $\pm$ 1 % boundary ripple of the uncompressed plasma (20 TF coils).

Fig. 8 $\langle ß_t \rangle$ -value after major radius compression as a function of compression ratio, for two types of electron heat conduction models.

Fig. 9 Ignition parameter $(P_{\alpha} - P_{loss})/P_{\alpha}$, determined 0.7 sec after compression as function of compression ratio, for two types of electron heat conduction models.

Fig. 10 Effect of improved spezies mix on $\langle \beta_t \rangle$ values after neutral injection and major radius compression, as a function of compression ratio.

Fig. 11a Effect of adjustment of neutral injection pulse length to the variation of pre-compression confinement time on $\langle \beta_t \rangle$ as a function of compression ratio.

11b Neutral injection pulse length variation used in the dashed line heating scenario of fig. 4a.

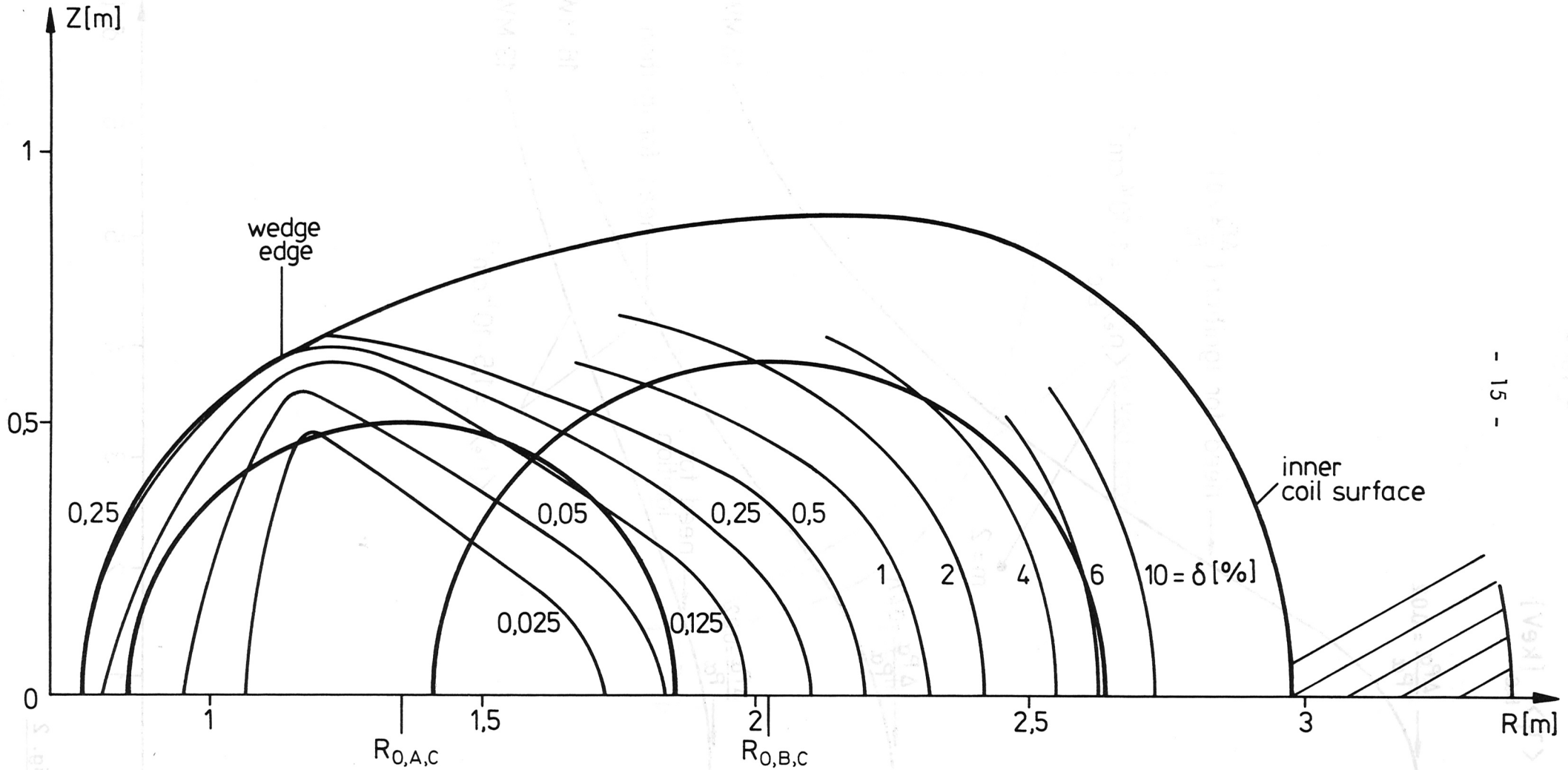
Z[m]
1
0,5
0
wedge
edge
inner
coil surface
0,25
0,05
0,25
0,5
1
2
4
6
10 = δ [%]
0,025
0,125
1
1,5
2
2,5
3
R[m]
R0,A,C
R0,B,C

Fig. 1

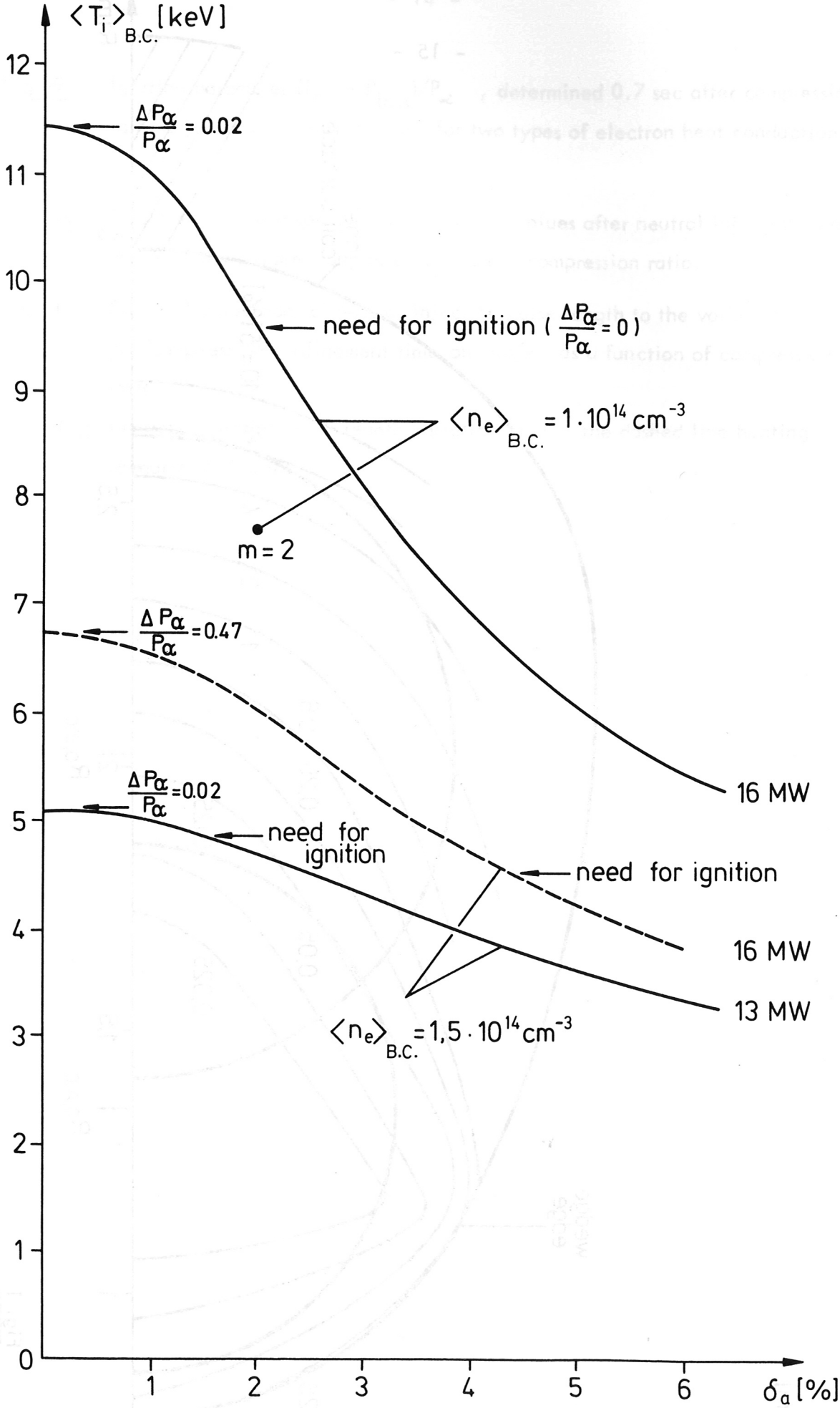
$\langle T_i \rangle_{B.C.}$ [keV]
12
11
10
9
8
7
6
5
4
3
2
1
0
$\frac{\Delta P_\alpha}{P_\alpha} = 0.02$
need for ignition ($\frac{\Delta P_\alpha}{P_\alpha} = 0$)
$\langle n_e \rangle_{B.C.} = 1 \cdot 10^{14}\,cm^{-3}$
m = 2
$\frac{\Delta P_\alpha}{P_\alpha} = 0.47$
$\frac{\Delta P_\alpha}{P_\alpha} = 0.02$
need for ignition
need for ignition
16 MW
16 MW
13 MW
$\langle n_e \rangle_{B.C.} = 1{,}5 \cdot 10^{14}\,cm^{-3}$
1
2
3
4
5
6
δ_α [%]

Fig. 2

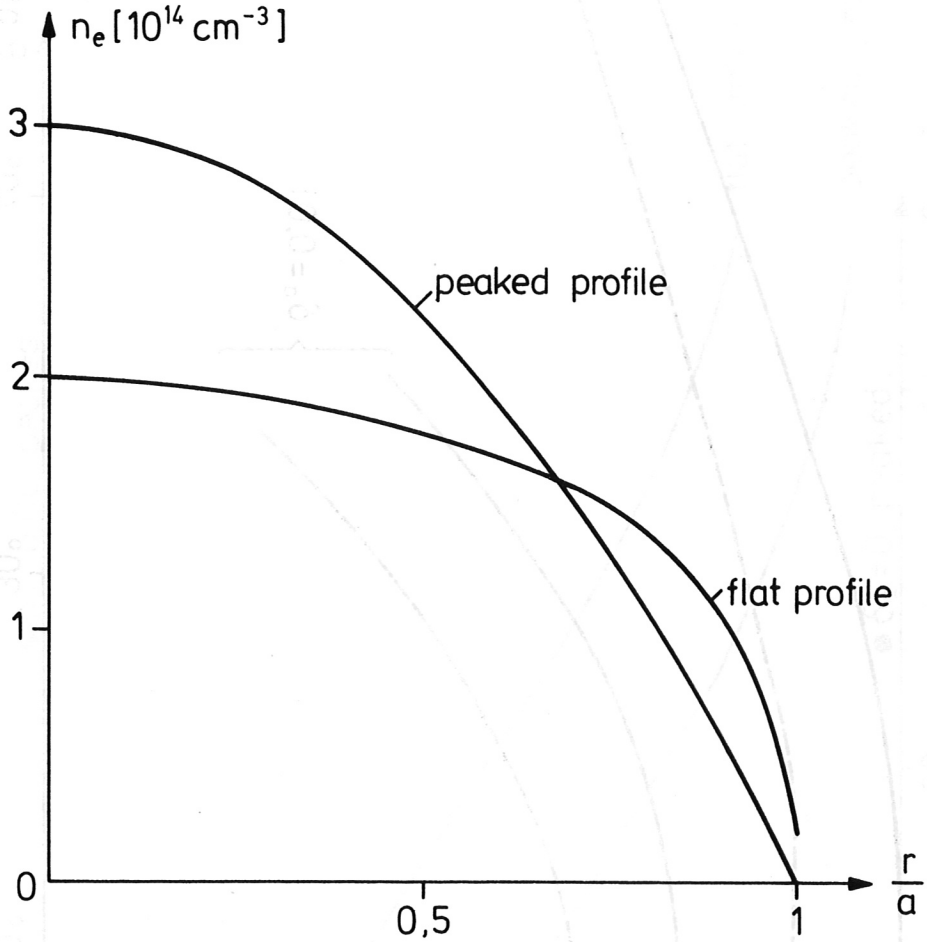

Fig. 3

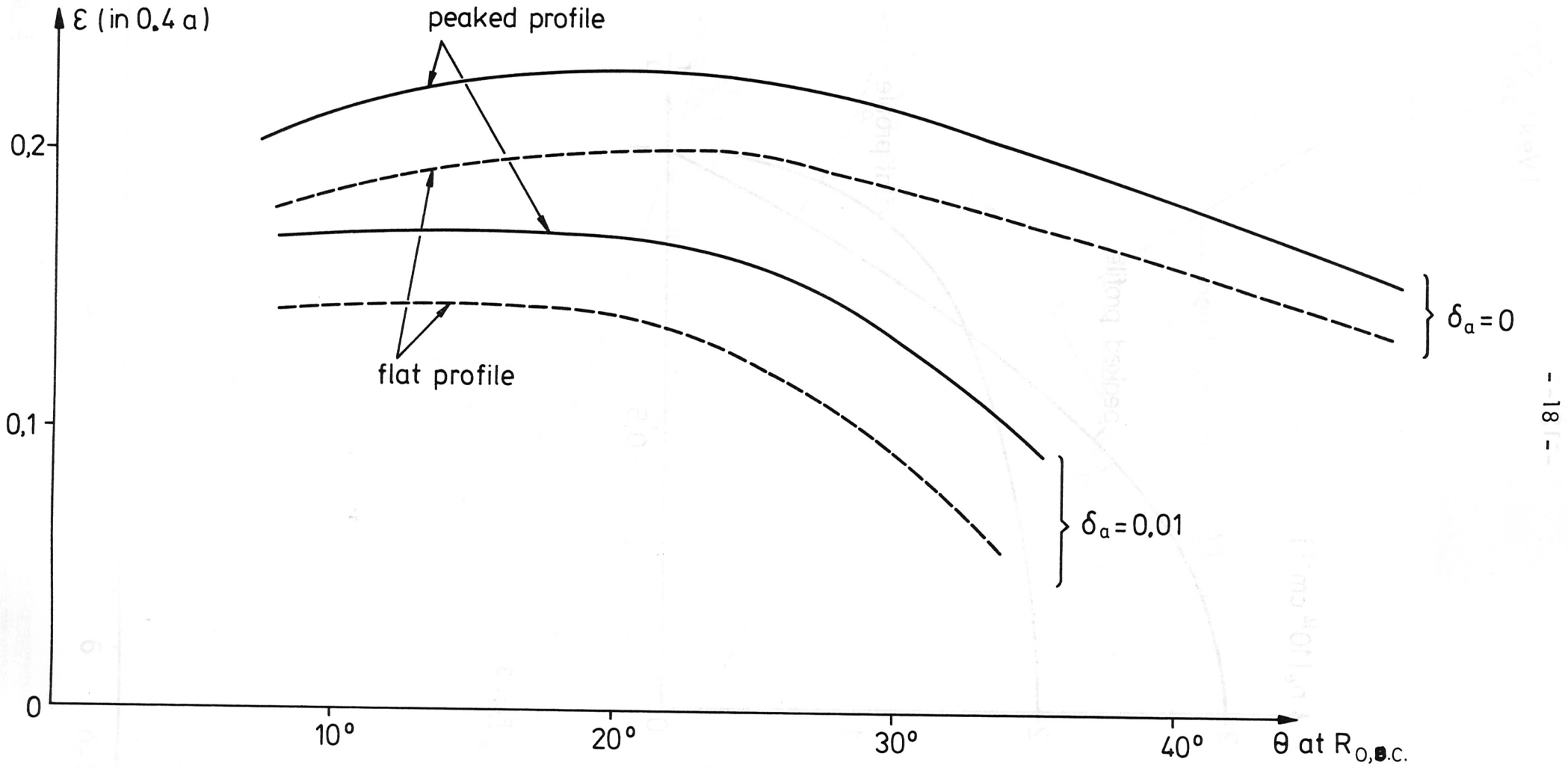
ε (in 0,4 a)
peaked profile
0,2
0,1
0
flat profile
δα = 0
δα = 0,01
10°
20°
30°
40°
θ at R0,B.C.

Fig. 4

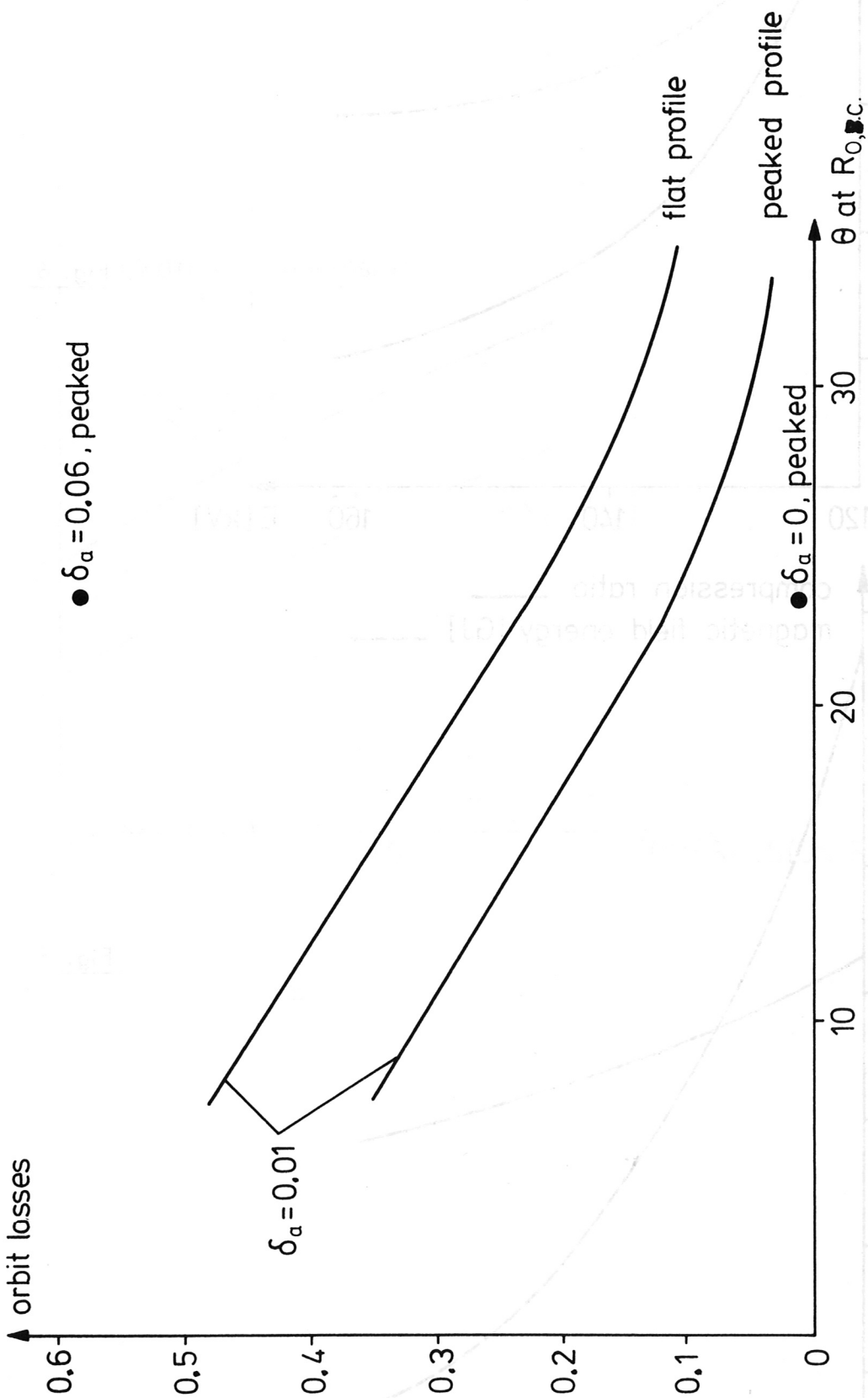
orbit losses
0,6
0,5
0,4
0,3
0,2
0,1
0
10
20
30
θ at R0,a.c.
δa = 0,06, peaked
δa = 0,01
δa = 0, peaked
flat profile
peaked profile

Fig. 5

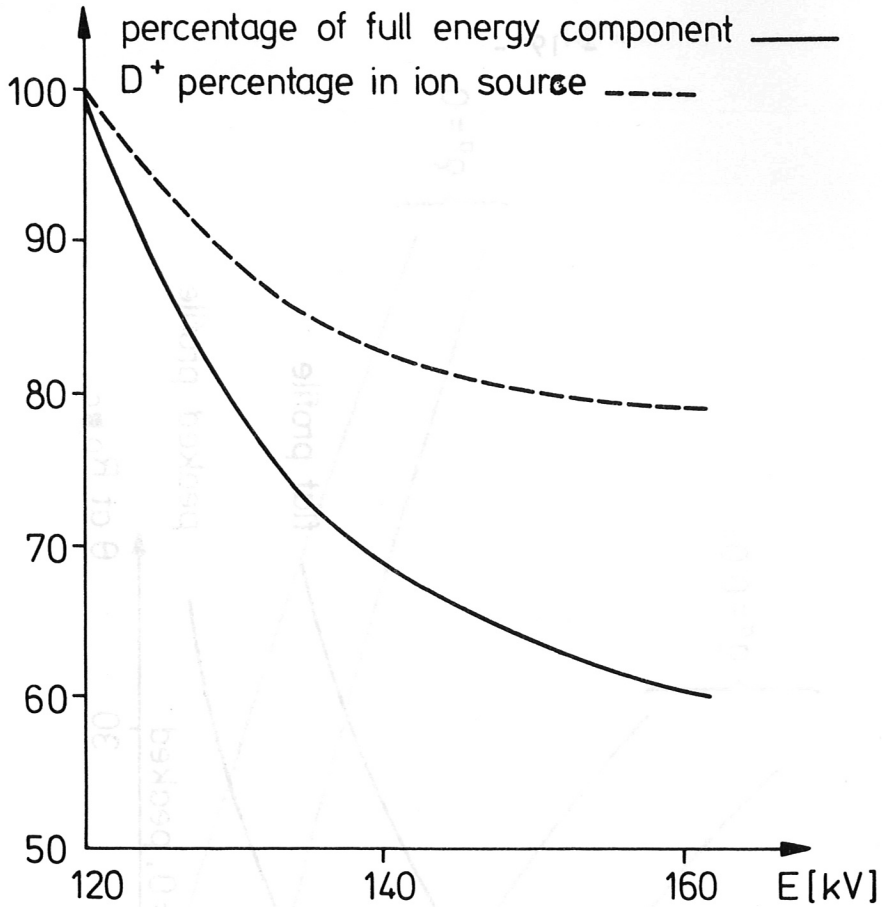
percentage of full energy component
D+ percentage in ion source
100
90
80
70
60
50
120
140
160
E [kV]

Fig. 6

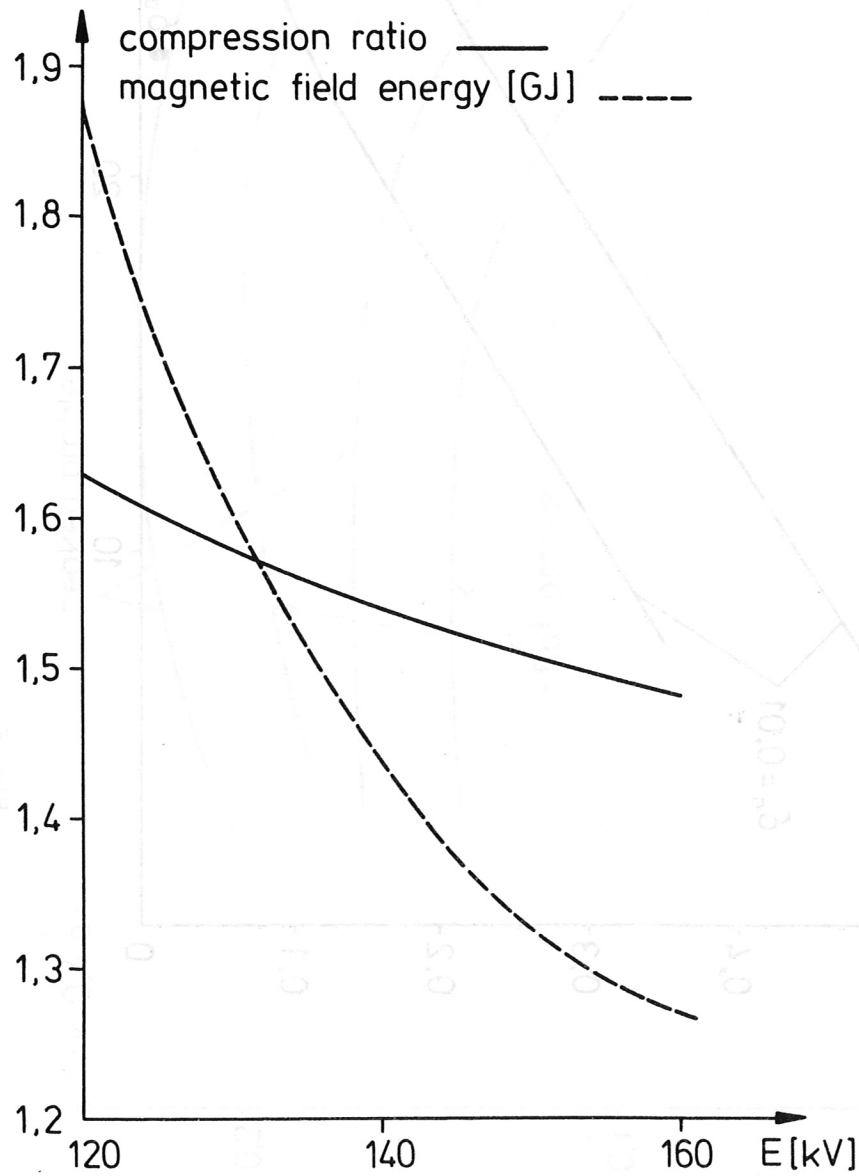
compression ratio
magnetic field energy [GJ]
1,9
1,8
1,7
1,6
1,5
1,4
1,3
1,2
120
140
160
E [kV]

Fig. 7

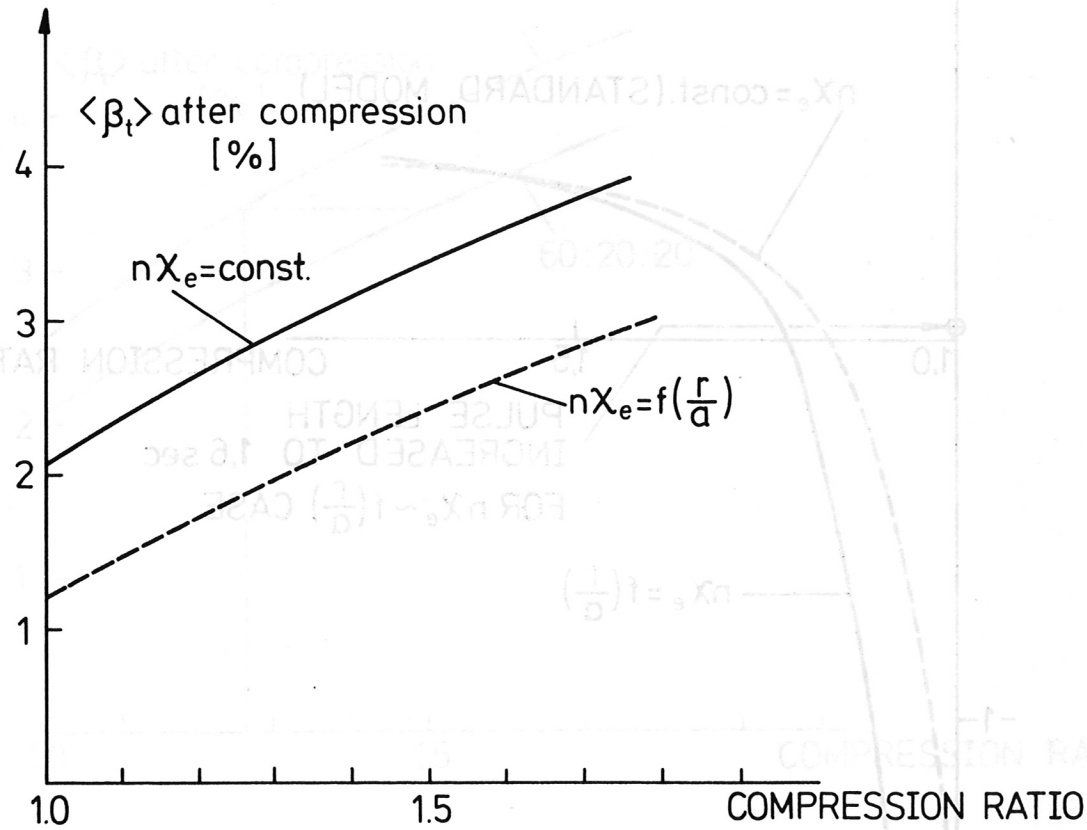
$\langle\beta_t\rangle$ after compression
[%]
4
3
2
1
$n\chi_e$=const.
$n\chi_e=f(\frac{r}{a})$
1.0
1.5
COMPRESSION RATIO

Fig. 8

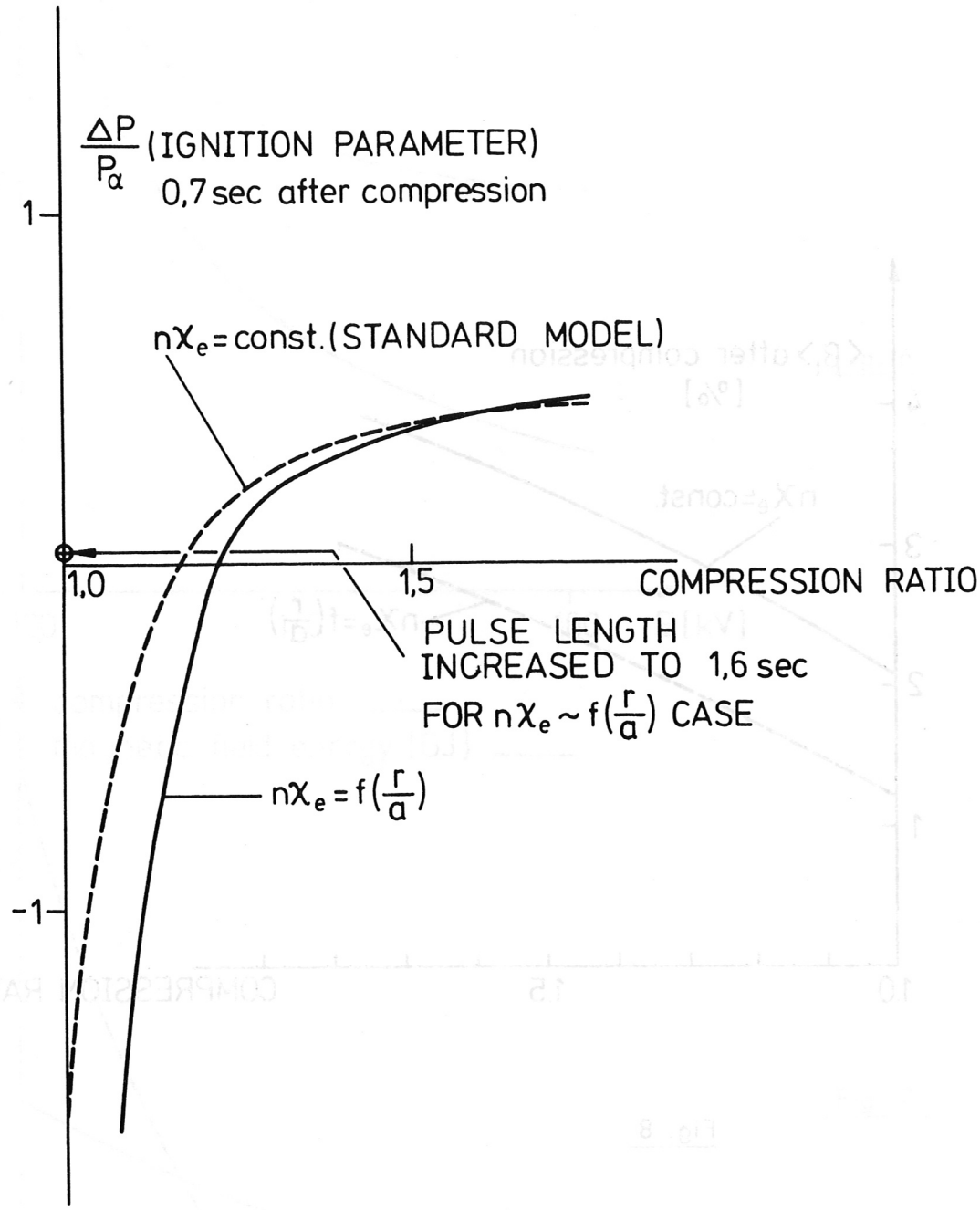
ΔP/Pα (IGNITION PARAMETER)
0,7 sec after compression
1
nχe = const. (STANDARD MODEL)
1,0
1,5
COMPRESSION RATIO
PULSE LENGTH
INCREASED TO 1,6 sec
FOR nχe ~ f(r/a) CASE
nχe = f(r/a)
-1

Fig. 9

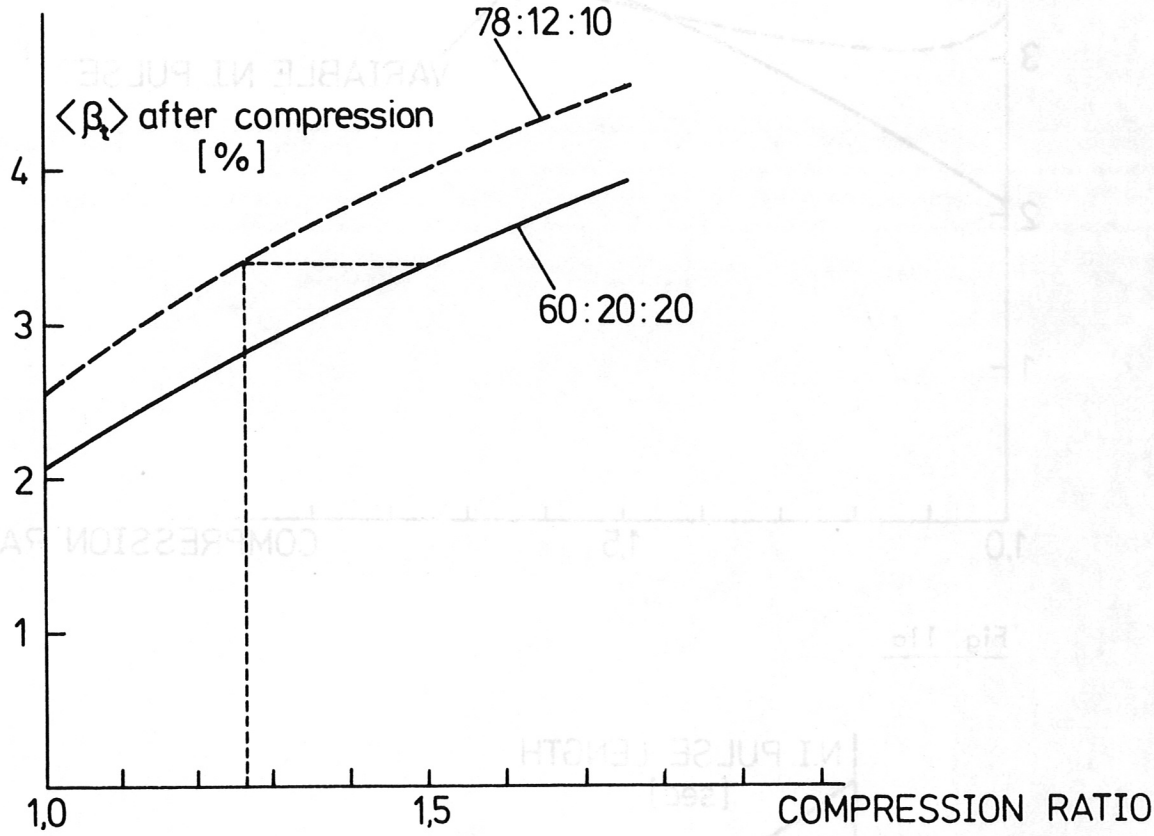
78:12:10
$\langle\beta_t\rangle$ after compression
[%]
4
3
2
1
60:20:20
1,0
1,5
COMPRESSION RATIO

Fig. 10

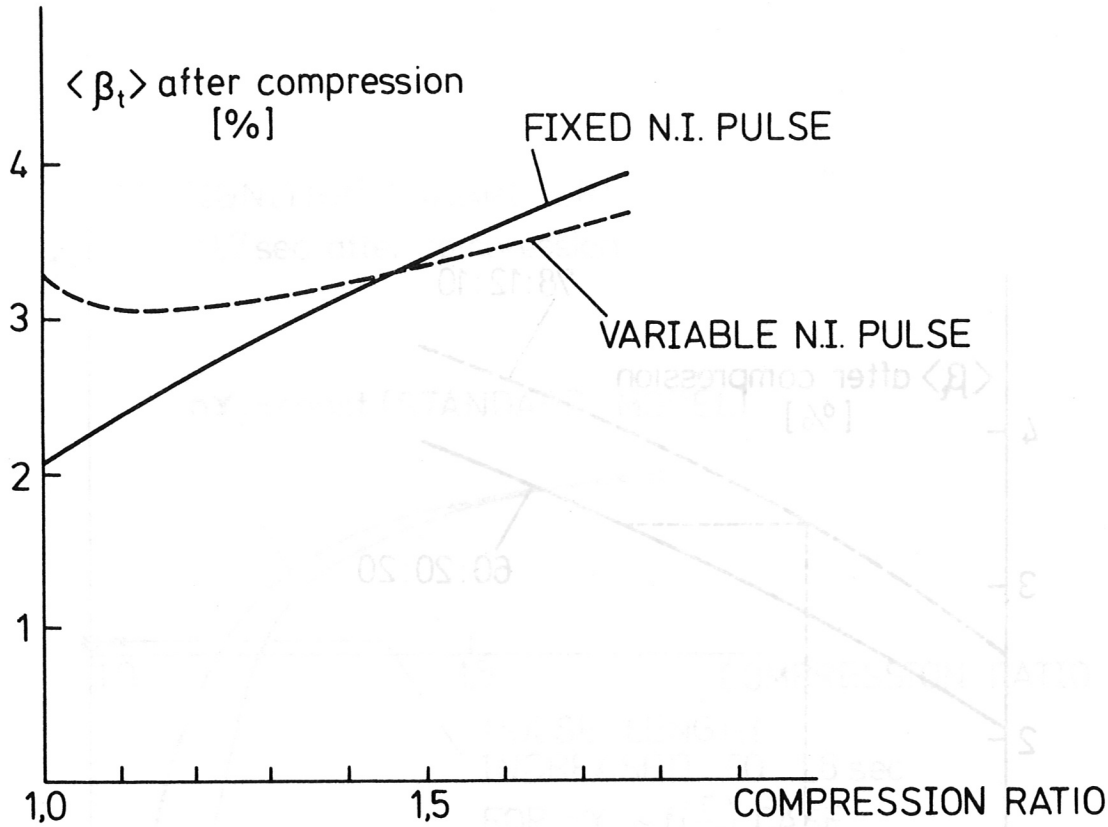

Fig. 11a

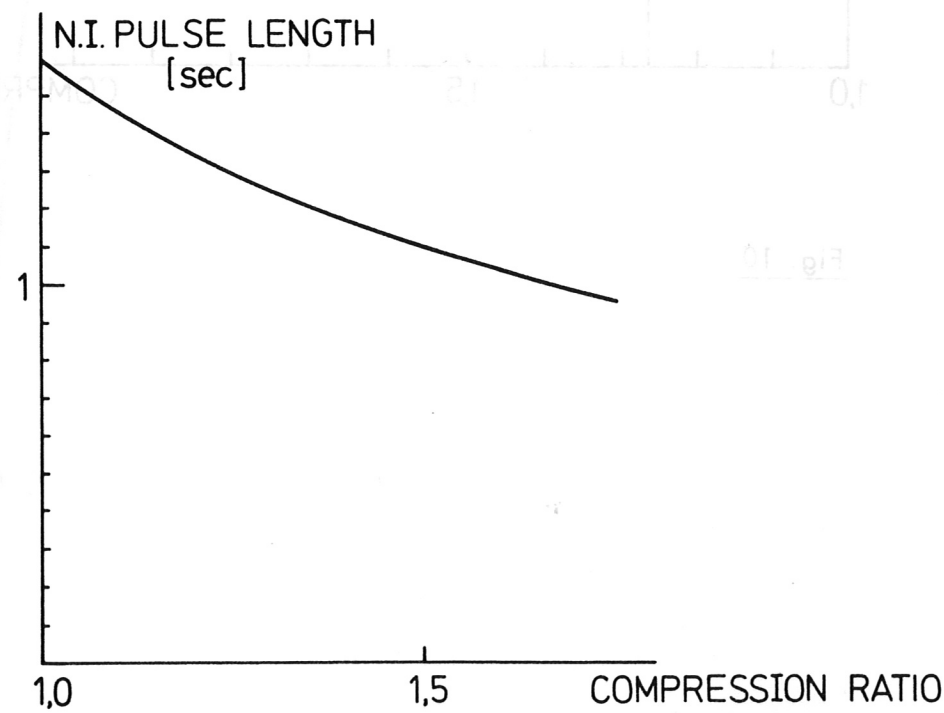

Fig. 11b